

# DNA–Protein Binding Force Chip

Philip M. D. Severin and Hermann E. Gaub\*

Force measurements provide new fundamental and complementary information on biomolecular interactions, particularly in the high and low affinity regimes, which may hardly be obtained otherwise.<sup>[1]</sup> We introduce a label free parallel format assay to quantify the binding forces in protein–DNA complexes on a chip in crowded environments. It employs arrays of molecular force balances with fluorescent read-out and fulfills all essential criteria for high throughput screening. The assay is fast, easy to operate and requires only a quantitative fluorescence microscope as instrumentation.

Despite years of intensive research, the need for a deeper understanding of protein–DNA interactions remains eminent.<sup>[2]</sup> A multitude of different techniques were introduced over the past years to characterize intrinsic affinities and dissociation constants in low throughput formats.<sup>[3]</sup> However, the growing complexity of the systems e.g. in epigenetics or systems biology, spurs the urgent need for precise and reliable high-throughput methods, which can provide large data sets not only on the qualitative level but moreover give quantitative information on the underlying biophysics of protein–DNA interactions.<sup>[2]</sup>

Conventional techniques measure protein–DNA interactions by comparing them with the energy of thermal excitations, e.g. by “counting” the number of proteins bound to DNA at different concentrations, or determine rates by measuring the kinetics of the return to equilibrium after a disturbance.<sup>[4–8]</sup> Weak interactions will thus result in fast off rates and may be missed in washing steps whereas strong interactions will result in off rates beyond the time span of the experiments.<sup>[9,10]</sup> These protein–DNA interactions are the result of forces between the binding partners, which promise higher accuracy when measured directly. Single molecule force techniques, like optical or magnetic tweezers or AFM, have successfully been used to quantify binding forces with superb precision, but none of these methods offers high throughput.<sup>[11–17]</sup> The lack of suitable methods to achieve a

high level of parallelization in force measurements was up to now the dominant bottleneck.

Recently, we introduced a comparative force assay, which employs molecular force probes (MFP) consisting of a reference complex as force sensor and labels for the fluorescent readout. We successfully used this assay to measure DNA–ligand binding in crowded and complex molecular environments. The format requires no labeling of the DNA binding ligand itself, and is applicable over a broad range of affinities (pM to mM).<sup>[18–22]</sup> Here, we present a binding force chip, which for simplicity we refer to as BiFo-Chip. It is a consequent miniaturization and parallelization, which uses an array of different MFPs to characterize the binding forces between DNA and proteins in a very sensitive manner. Parallel arrays of MFPs with different reference complexes are used acting as analog to digital converters for the binding forces under investigation. The size of the MFP spots was reduced to a diameter of approximately 20  $\mu\text{m}$ , providing the feature density needed for high-throughput applications.

As depicted in **Figure 1**, the MFPs used in this study are anchored covalently via one DNA strand to the (lower) chip surface at a density of around  $10^4$  MFPs per  $\mu\text{m}^2$ . Each MFP is comprised of three DNA strands. These three DNA strands form two DNA duplexes coupled in series, a 20 bp target duplex (upper duplex, red), as well as a reference duplex with 15 bp to 50 bp (lower duplex, black and blue). The middle DNA strand carries Cy5 as a fluorescent marker while the other strand of the target duplex has a Cy3 fluorescence marker at one end and biotin at the other end for coupling via streptavidin to the upper surface, which consists of an elastomer stamp with a square pattern of drainage channels. Upon separation of the two surfaces, a force builds up gradually in each individual MFP until either the target duplex or the reference duplex ruptures. Subsequently, the ratio of ruptured target to reference duplexes is read out on the lower surface with a quantitative fluorescence microscope and analyzed to calculate the normalized fluorescence (NF). The NF is defined as the ratio of broken target bonds to the total number of MFPs that were under load. Accordingly, the NF is a quantitative measure which describes the relative mechanical stability between the target and reference DNA duplex of a MFP. The color-coded fluorescence maps of the two experiments (see Figure 1) show clearly that in the symmetric case NF is close to 0.5 with small local variations, whereas the asymmetric MFP shows a NF of close to 1.0. It should be noted here that the physical force measurement - the comparison of the sample force with a reference force - occurs simultaneously in all  $10^{11}$  MFPs on the  $\text{cm}^2$  chip within fractions of a second in the moment when the stamp is removed,

Prof. H. E. Gaub, P. M. D. Severin  
Lehrstuhl für Angewandte Physik and Center for  
Nanoscience (CeNS), Ludwig-Maximilians-Universität  
Amalienstrasse 54, 80799 Munich, Germany  
E-mail: gaub@physik.uni-muenchen.de

Prof. H. E. Gaub, P. M. D. Severin  
Munich Center For Integrated Protein Science (CIPSM)  
Ludwig-Maximilians-Universität  
Butenandtstrasse 5-13, 81377 Munich, Germany



DOI: 10.1002/sml.201201088

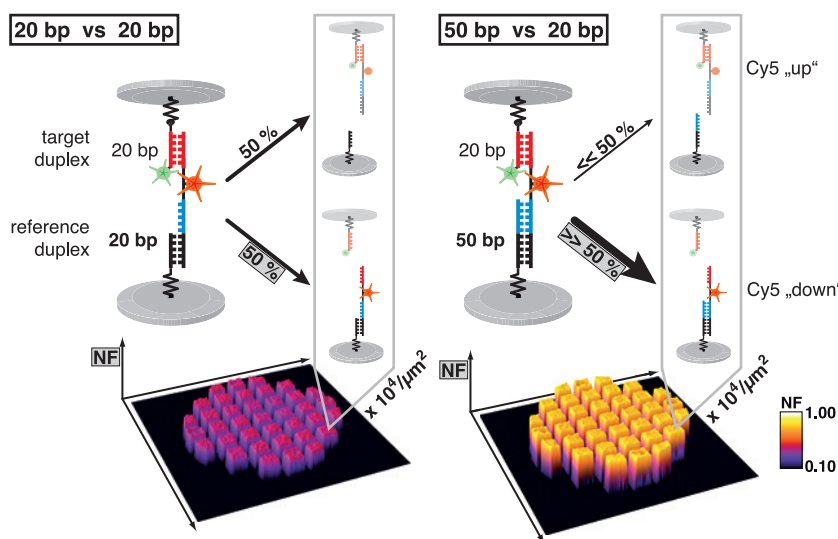


**Figure 1.** Schematics of a BiFo-Chip. The MFPs are composed of two dsDNA duplexes, a target duplex and a reference duplex, which are coupled in series and connected between two surfaces. After separation of the surfaces: 20 bp reference duplex versus 20 bp target duplex results in a normalized fluorescence (NF) of 0.5 (left), while 50 bp reference duplex versus 20 bp target duplex results in a  $NF \gg 0.5$ . In the NF image the contacted and probed areas are clearly visible (microstructure of 100  $\mu\text{m} \times 100 \mu\text{m}$  squares).

best understood by analogy to a simple balance, where the gravitational force of an object is compared to that of a reference and where more and more counterweights are added until finally the difference converges to zero. In the case of BiFo-Chip, we design the target duplex such that it will bind to the analyte, whereas the reference duplex does not. We now compare the binding force of the analyte-complexed target duplex with the binding force of the reference duplexes. On different spots of the array, we offer MFPs with different reference duplex lengths. We offer, so to say, an array of balances with different counterweights and identify that spot where  $NF = 0.5$ , which means that the difference is zero. Thereby, it must be taken into account that the reference force is not only depending on the reference duplex length but also on the reference duplex composition of A-T and G-C base pairs. A demonstration of the wide range of applications of BiFo-Chip

while the readout via fluorescence may occur serially at a much later time e.g. via slow scanning.

In **Figure 2**, the implementation of the BiFo-Chip at different length scales is demonstrated in a series of representative experiments. The BiFo-Chip utilizes eight different reference duplexes ranging in 5 bp steps from 15 bp through 50 bp and the target duplex has a length of 20 bp. While in **Figure 2(a)** a BiFo-Chip experiment was performed as proof of principle with 1 mm (diameter) spots per type of reference duplex, in **Figure 2(b)** a NF-image section of a BiFo-microarray with identical units is shown, and **Figure 2(c)** presents a high resolution NF-image of a single BiFo-microarray unit. A comparison of the NF-values for the BiFo-Chip at different length scales is illustrated in **Figure 2(d)**. In summary, fluctuations in the NF values are virtually independent of the feature size, which means that we can achieve even further miniaturization with no degradation in readout accuracy. The dashed curve is the analytical solution based on the Bell-Evans model (Supporting Information).<sup>[23,24]</sup>

The central idea of the BiFo-Chip as a sensor for DNA-ligand interactions is based on a zero-compensation measurement, a concept which is widely used for extremely sensitive measurements and is

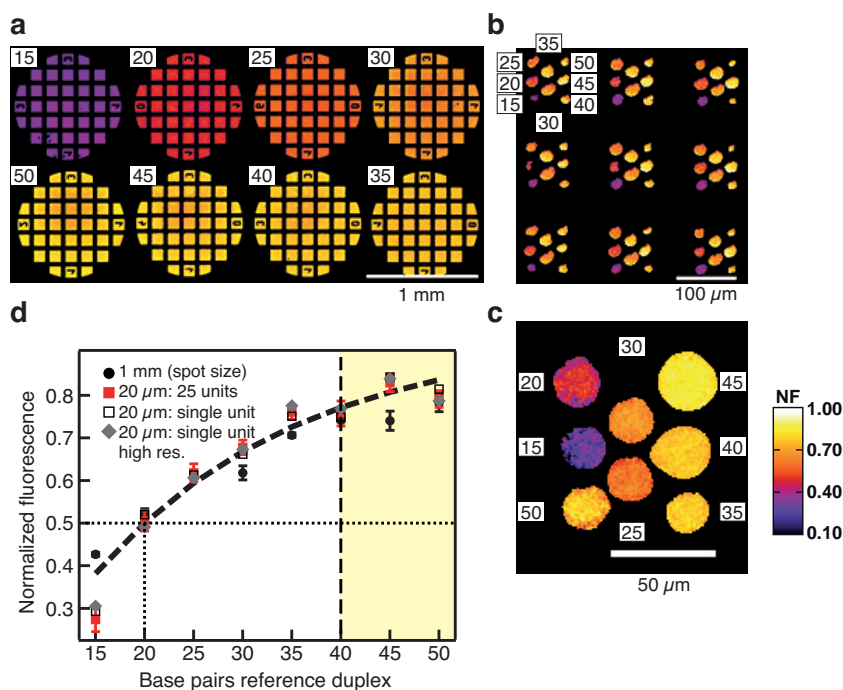


**Figure 2.** Implementation of the BiFo-Chip. Numbers in white boxes specify the reference duplex length in base pairs. (a) NF images of a representative BiFo-Chip experiment with a spot-size of 1 mm per type of MFP. (b) BiFo-microarray. (c) NF high-resolution image of a single BiFo-unit. (d) Graph of the mean NF against the reference duplex length. With growing reference duplex length the NF increases from approx. 0.35 at 15 bp to approx. 0.80 at 50 bp. Above a length of 40 bp (light yellow), the rupture forces of the DNA-oligomers reach significantly into B-S transition of DNA at 65 pN, which results in a plateau in NF. Black filled circle: NF-mean and s.e.m. of 32 spots of 1 mm diameter (as in (a)); filled red square: NF-mean and s.e.m. of 25 units BiFo-microarray; black empty square: single, typical BiFo-microarray unit; grey filled diamond: high-res. NF-image (as in (c)).

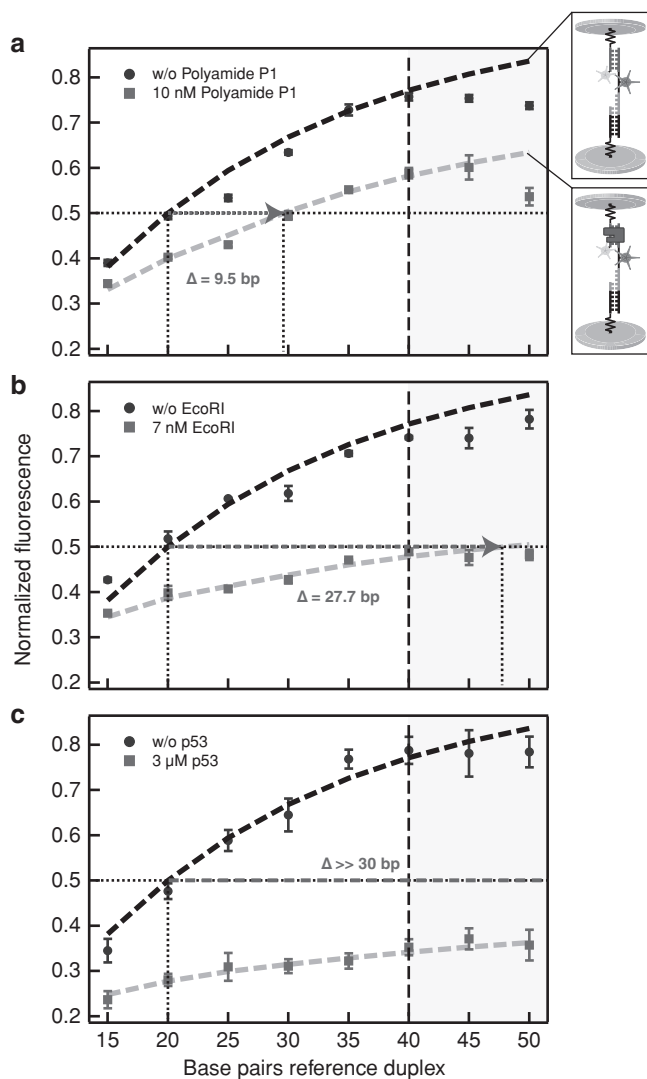


**Figure 3.** Characterization of DNA-binders via the BiFo-Chip. (a) Polyamide P1 (b) Endonuclease EcoRI (c) Transcription factor p53 DNA-binding domain. In all three cases the target duplex carries a specific recognition sequence for the corresponding ligand, while the reference duplex does not. The complex of ligand and target DNA duplex exhibits a higher unbinding force as the target duplex itself. Thus, the NF is shifted to a lower value. The dashed curves represent the analytical solution based on the Bell-Evans 2-state model.

as a force sensor for three different types of DNA binders (pyrrole-imidazole hairpin polyamide, restriction endonuclease and transcription factor) is given in **Figure 3**. The target duplexes contain the corresponding target sequences, while the reference duplexes are lacking any binding site (alternatively L-DNA may be chosen for the reference duplexes). The BiFo-chip was incubated with the corresponding analyte at a concentration at least two orders above the dissociation constant. A description of the DNA oligomers, which were used to assemble the  $3 \times 8$  different MFPs, can be found in the Supporting Information.

Figure 3(a) shows the interaction of a pyrrole-imidazole hairpin polyamide (P1), which is programmed to bind to the six-base-pair DNA sequence 5'-TGGTCA-3'.<sup>[19,20]</sup> Figure 3(b) demonstrates the interaction of a type II

restriction endonuclease (EcoRI). EcoRI binds as a dimer to the palindromic DNA target site 5'-GAATTC-3' without enzymatic activity in the absence of  $\text{Mg}^{2+}$  ion cofactor. Finally, Figure 3(c) shows the interaction of the tumor suppressor protein p53 DNA-binding domain with the DNA consensus sequence  $\text{CON}2 \times 5$ .<sup>[25]</sup> The p53 protein belongs to the family of transcription factors. The DNA-binding domain of p53 binds cooperatively as a dimer to  $\text{CON}2 \times 5$ . Thereby the ligands cover approximately from 6 to 12 bp center positioned on the 20 bp target duplex, leaving several bp free to each side of the target duplex. In Figure 3, dark blue circles represent the measurement without ligand and light blue squares the equivalent experiment with ligand. In all three cases the NF drops to a lower value in the presence of the ligand. The red dashed line at  $\text{NF} = 0.5$  marks the difference in mechanical stability caused by the ligand-DNA interaction. The dashed gray curve originates also from the 2-state model but should not be over-interpreted, since a 2-state model omits the details of the energy landscape that must be overcome in the rupture process and therefore represents the rupture process of the ligand-DNA complex only in a zero order approximation.

If needed, the absolute values of the forces in Figure 3 in units of pN may be obtained by a comparison with AFM-based single molecule force spectroscopy data. At a loading rate of  $10^5 \text{ pN s}^{-1}$  the 10 bp duplex ruptures at 45 pN and the 30 bp at 54 pN.<sup>[26]</sup> More importantly for the discussion here, and also more intuitive, is the relative comparison. Figure 3(a) illustrates that the polyamide stabilizes the DNA duplex in the same way as an extension of the duplex by 9.5 bp would do, and the interaction of EcoRI stabilizes it even more, equivalent to an extension of the duplex by 27.7 bp. To match a p53-DNA complex, one would have to extend the reference duplex by more than 30 bp. To quantify even strong binders like p53 more precisely, one might want to extend the range of reference forces. This can be accomplished, e.g. by adding one, two or more binding sites for a certain polyamide into a reference duplex. Hereby it is possible to use L-DNA reference duplexes and polyamides, which bind exclusively to L-DNA. Thus any interference of the polyamide with the investigated ligand is avoided. Alternatively, synthetic nucleic acids like PNA may be included in the reference complex, increasing its stability. It should be noted here, that this method not only provides interaction forces, but has also the potential to determine the dissociation constant in one measurement when the binding stoichiometry is known and the titration curve is determined for one target sequence.<sup>[27]</sup> In addition, BiFo-Chip measurements with different pulling velocities may also provide lifetimes and characteristic interaction distances of the prominent activation barriers of protein-DNA interactions on a high-throughput level, which is not possible with binding affinity assays and until now was only accessible with force-based techniques.<sup>[27]</sup> Furthermore, the BiFo-Chip is by principle not affected by unspecific binding of the protein to the chip surface, since the BiFo-Chip detects the interaction between DNA and ligand and not merely the presence of ligand. Therefore, the BiFo-Chip does not exhibit stringency washing or background problems as do binding affinity assays.<sup>[22]</sup>

In summary, we have demonstrated the first high-throughput format for biomolecular force measurements. We characterized with this assay the interaction forces of three different types of unlabeled analytes. This force-based method enables the measurement of new types of interaction parameters that thus far have been inaccessible for high-throughput techniques.

## Experimental Section

The fabrication of the BiFo-Chip and the PDMS stamp can be found in the Supporting Information.

**Ligands and Incubation:** Prior to the measurement, the DNA-chips were incubated with the corresponding buffer solution. Synthesis, composition and function of the pyrrole-imidazole hairpin polyamide P1 have been described previously.<sup>[19,28]</sup> Polyamide measurements were performed in 1× PBS containing 10 nM P1. Commercial grade EcoRI (32 kDa per monomer, 2 × 10<sup>6</sup> U mg<sup>-1</sup> specific activity, 100 000 U ml<sup>-1</sup> stock concentration) was purchased from NEB and used in the experiment directly without further purification at a final concentration of 7 nM. EcoRI buffer solution is composed of 10 mM Hepes, 50 mM DTT, 100 mg ml<sup>-1</sup> BSA, 170 mM NaCl and 1 mM EDTA (pH of 7.6). Wild-type p53DBD consists of residues 94–312 of human p53. Expression and purification of human p53DBD has been described elsewhere.<sup>[25]</sup> The p53DBD buffer is composed of 50 mM potassium phosphate, pH 6.8, 50 mM KCl and 5 mM DTT. The p53DBD measurements were performed at a concentration of 3 μM. All control measurements were carried out with the same buffer solutions but without ligand. Each DNA-chip was incubated for at least 1 h prior to measurement. All experiments were performed at room temperature.

**Contact process, readout and analysis:** A detailed description of the measurement process can be found in a previous paper.<sup>[22]</sup> Briefly, a custom-built contact device mounted on a fluorescence microscope controls contact and separation between PDMS stamp and DNA-chip via a closed-loop piezoelectric actuator. At first, DNA-chip and the soft PDMS stamp are apart. Cy5 is excited with a LED (627 nm peak wavelength) and the fluorescence signal ( $F_A^A$ ) of the DNA-chip is measured. Then Cy3 is excited with a second LED (530 nm peak wavelength) and the fluorescence signal ( $F_D^A$ ) of Cy5 is measured. The PDMS stamp is lowered with the piezoelectric actuator until both surfaces are brought into contact, allowing to connect strand 3 of the MFPS to the streptavidin on the PDMS surface (complex formation of biotin • streptavidin). After 10 min the PDMS stamp is moved upwards to separate the surfaces with a retract velocity of 5 μm s<sup>-1</sup>. The applied PDMS stamp retraction velocity of 5 μm s<sup>-1</sup> is chosen that on the one hand the timescale of force probing is small compared to the timescale of inverse dissociation rate and on the other hand the deformation of the elastic PDMS stamp is not influencing the measurement distinctly. Afterwards,  $F_A^A$  and  $F_D^A$  are read out a second time. For each region of interest the four fluorescence images ( $F_A^A$  and  $F_D^A$  before contact and after separation) are analyzed to determine the normalized fluorescence intensity with custom-build analysis software written in LabVIEW.

## Supporting Information

Supporting Information is available from the Wiley Online Library or from the author.

## Acknowledgements

The authors are grateful to P.B. Dervan for providing the pyrrole-imidazole hairpin polyamide and to J. Buchner for providing human p53. The authors thank J. Buchner, M. Retzlaff and D. Ho for helpful discussions. P.S. was supported by the Elite Network of Bavaria (IDK-NBT) with a doctoral fellowship. Financial support was provided by the Deutsche Forschungsgemeinschaft, the Nanosystems Initiative Munich and the German Science Foundation (SFB 863).

- [1] C. Bustamante, Y. Chemla, N. Forde, D. Izhaky, *Annu. Rev. Biochem.* **2004**, *73*, 705–748.
- [2] D. Evanko, *Nat. Meth.* **2011**, *8*, 619.
- [3] R. Nutiu, R. C. Friedman, S. Luo, I. Khrebtukova, D. Silva, R. Li, L. Zhang, G. P. Schroth, C. B. Burge, *Nat. Biotechnol.* **2011**, *29*, 659–664.
- [4] M. F. Berger, A. A. Philippakis, A. M. Qureshi, F. S. He, P. W. Estep, M. L. Bulyk, *Nat. Biotechnol.* **2006**, *24*, 1429–1435.
- [5] M. L. Bulyk, *Curr. Opin. Biotechnol.* **2006**, *17*, 422–430.
- [6] V. R. Iyer, C. E. Horak, C. S. Scafe, D. Botstein, M. Snyder, P. O. Brown, *Nature* **2001**, *409*, 533–538.
- [7] T. I. Lee, N. J. Rinaldi, F. Robert, D. T. Odom, Z. Bar-Joseph, G. K. Gerber, N. M. Hannett, C. T. Harbison, C. M. Thompson, I. Simon, J. Zeitlinger, E. G. Jennings, H. L. Murray, D. B. Gordon, B. Ren, J. J. Wyrick, J.-B. Tagne, T. L. Volkert, E. Fraenkel, D. K. Gifford, R. A. Young, *Science* **2002**, *298*, 799–804.
- [8] S. Mukherjee, M. F. Berger, G. Jona, X. S. Wang, D. Muzzey, M. Snyder, R. A. Young, M. L. Bulyk, *Nat. Genet.* **2004**, *36*, 1331–1339.
- [9] P. M. Fordyce, D. Gerber, D. Tran, J. Zheng, H. Li, J. L. Murray, S. R. Quake, *Nat. Biotechnol.* **2010**, *28*, 970–976.
- [10] S. J. Maerkl, S. R. Quake, *Science* **2007**, *315*, 233–237.
- [11] F. Kuehner, L. Costa, P. Bisch, S. Thalhammer, W. Heckl, H. E. Gaub, *Biophys. J.* **2004**, *87*, 2683–2690.
- [12] S. Smith, Y. Cui, C. Bustamante, *Science* **1996**, *271*, 795–799.
- [13] T. Strick, J. Allemand, D. Bensimon, V. Croquette, *Biophys. J.* **1998**, *74*, 2016–2028.
- [14] F. Bartels, B. Baumgarth, D. Anselmetti, R. Ros, A. Becker, *J. Struct. Biol.* **2003**, *143*, 145–152.
- [15] S. J. Koch, A. Shundrovsky, B. C. Jantzen, M. D. Wang, *Biophys. J.* **2002**, *83*, 1098–1105.
- [16] R. Merkel, P. Nassoy, A. Leung, K. Ritchie, E. Evans, *Nature* **1999**, *397*, 50–53.
- [17] V. T. Moy, E. Florin, H. E. Gaub, *Science* **1994**, *266*, 257–259.
- [18] C. H. Albrecht, K. Blank, M. Lalic-Mülthaler, S. Hirler, T. Mai, I. Gilbert, S. Schiffmann, T. Bayer, H. Clausen-Schaumann, H. E. Gaub, *Science* **2003**, *301*, 367–370.
- [19] C. Dose, D. Ho, H. E. Gaub, P. B. Dervan, C. H. Albrecht, *Angew. Chem. Int. Ed.* **2007**, *46*, 8384–8387.
- [20] D. Ho, C. Dose, C. H. Albrecht, P. M. D. Severin, K. Falter, P. B. Dervan, H. E. Gaub, *Biophys. J.* **2009**, *96*, 4661–4671.
- [21] D. Ho, K. Falter, P. M. D. Severin, H. E. Gaub, *Anal. Chem.* **2009**, *81*, 3159–3164.
- [22] P. M. D. Severin, D. Ho, H. E. Gaub, *Lab Chip* **2011**, *11*, 856–862.

- [23] G. Bell, *Science* **1978**, *200*, 618–627.
- [24] E. Evans, K. Ritchie, *Biophys. J.* **1999**, *76*, 2439–2447.
- [25] A. Dehner, C. Klein, S. Hansen, L. Müller, J. Buchner, M. Schwaiger, H. Kessler, *Angew. Chem. Int. Ed.* **2005**, *44*, 5247–5251.
- [26] T. Strunz, K. Oroszlan, R. Schäfer, H. J. Güntherodt, *Proc. Natl. Acad. Sci. USA* **1999**, *96*, 11277–11282.
- [27] S. J. Koch, M. D. Wang, *Phys. Rev. Lett.* **2003**, *91*, 028103.
- [28] D. Herman, E. Baird, P. B. Dervan, *J. Am. Chem. Soc.* **1998**, *120*, 1382–1391.

Received: May 18, 2012  
Published online: August 9, 2012

Copyright WILEY-VCH Verlag GmbH & Co. KGaA, 69469 Weinheim, Germany, 2012.

NANO MICRO  
**small**

Supporting Information

for *Small*, DOI: 10.1002/smll.201201088

DNA–Protein Binding Force Chip

*Philip M. D. Severin and Hermann E. Gaub\**

## Supporting Information

### DNA-protein binding force chip

*Philip M. D. Severin, and Hermann E. Gaub\**

[\*] Prof. H. E. Gaub, P. M. D. Severin

Lehrstuhl für Angewandte Physik and Center for Nanoscience (CeNS), Ludwig-Maximilians-Universität

Amalienstrasse 54, 80799 Munich (Germany)

Munich Center For Integrated Protein Science (CIPSM), Ludwig-Maximilians-Universität, Butenandtstrasse 5-13, 81377 Munich (Germany)

E-mail: [gaub@physik.uni-muenchen.de](mailto:gaub@physik.uni-muenchen.de)

#### ***1. Fabrication of the BiFo-chip (Bottom surface)***

The DNA-chip has been assembled as described previously except for some minor modifications described here.<sup>[1]</sup> DNA oligomers were purchased HPLC grade from IBA GmbH (Goettingen, Germany). Each MFP is composed of three DNA oligomers **1**, **2** and **3**. These 3 DNA strands form 2 hybridized dsDNA duplexes, **1 • 2** and **2 • 3**, which are coupled in series via DNA oligomer **2**. Thereby, DNA oligomer **1** is covalently linked to the glass slide. DNA oligomer **3** is modified with biotin in order to form a link to the top surface (PDMS stamp) after contact. DNA oligomer **1** has an amine-modification at the end of the spacer, which allows covalent linkage to aldehyde-functionalized glass slides (Schott GmbH, Jena, Germany). For the 1 mm spot size DNA-chip, we spotted 1  $\mu$ l drops of 5 $\times$  SSC (saline

sodium citrate; Sigma-Aldrich GmbH, Munich, Germany) containing 25  $\mu\text{M}$  oligomer **1** on the aldehyde slide in a  $4 \times 4$  pattern and incubated the slide in a saturated NaCl ddH<sub>2</sub>O atmosphere overnight.

For the production of BiFo-microarrays, we deposited the same DNA oligomer **1** solution on the glass slide with a microplotter (GIX, Sonoplot, Middleton, USA). A standard glass capillary (World Precision Instruments, Inc.) with an inner diameter of 5  $\mu\text{m}$  was used, which resulted in spots of the diameter of around 20  $\mu\text{m}$  on the glass slide (dispenser voltage 2 V and 0.1 s dispensing time). The spots were deposited in a hexagonal grid with a 30  $\mu\text{m}$  spot-to-spot distance at a controlled humidity of 65%.

Afterwards, we washed the slide with ddH<sub>2</sub>O containing 0.2% sodium dodecyl sulfate (SDS; VWR Scientific GmbH, Darmstadt, Germany) and thoroughly rinsed it with ddH<sub>2</sub>O. Then, we reduced the resulting Schiff bases with 1% aqueous NaBH<sub>4</sub> (VWR Scientific GmbH, Darmstadt, Germany) for 90 min. Subsequently, the slide was washed with 1 $\times$  SSC and thoroughly rinsed with ddH<sub>2</sub>O. In order to reduce nonspecific binding, the slide was blocked in 1 $\times$  SSC containing 4% bovine serum albumin (BSA; Sigma-Aldrich GmbH, Munich, Germany) for 20 min. The 100 nm Cy5-modified oligomer **2** and 200 nm biotin-modified oligomer **3** were hybridized to the latter for 30 min, completing the **1 • 2 • 3** complex on the glass slide. After incubation with DNA oligomer **2** and **3**, the slides were washed with a self-made fluidic system driven by a multi-channel peristaltic pump (Ismatec GmbH, Wertheim-Mondfeld, Germany) to remove any unspecific bound DNA oligomers. The slide was rinsed subsequently with 2 $\times$  SSC, 0.2 $\times$  SSC containing 0.1% Tween 20 (VWR Scientific GmbH, Darmstadt, Germany) and 1 $\times$  PBS each with 50 ml in 5 min. For the BiFo-microarray it is also possible, to deposit the mixture of oligomer **2** and **3** directly with the microplotter. In this case the glass slide remains fixed in the microplotter in order to keep the position calibration between capillary and slide, while the washing steps are performed.

## ***2. Fabrication of the PDMS stamp (Top surface)***

The stamp consists of polydimethylsiloxane (PDMS) and was fabricated and functionalized on the surface as described previously.<sup>[2, 3]</sup> Briefly summarized, the PDMS stamps were cut into a  $4 \times 4$  or a single pillar arrangement. Each pillar has a diameter and height of 1 mm, and is furnished with a microstructure on the flat surface: quadratic pads with a side length of 100  $\mu\text{m}$  are separated by 41  $\mu\text{m}$  wide and 5  $\mu\text{m}$  deep trenches, which allow the liquid drainage during the contact and separation process. For surface functionalization, the PDMS was

activated overnight in 12.5% hydrochloric acid and subsequently derivatized with (3-glycidoxypropyl)-trimethoxysilane (ABCR, Karlsruhe, Germany) to generate epoxide groups. NH<sub>2</sub>-PEG-Biotin (3400 g mol<sup>-1</sup>; Rapp Polymere, Tuebingen, Germany) was melted at 80 °C, and ~1 ml was spotted on each pillar followed by overnight incubation in argon atmosphere at 80 °C. The excess polymers were thoroughly removed with 80 °C hot ddH<sub>2</sub>O. Shortly before the experiment, the PDMS was incubated for 120 min with a 1× PBS containing 0.4% BSA and 1 mg ml<sup>-1</sup> streptavidin (Thermo Fisher Scientific, Bonn, Germany). Lastly, the PDMS was rinsed with 1× PBS containing 0.1% Tween 20 and then gently dried under N<sub>2</sub> gas flow.

### ***3. Oligomer sequences***

Oligonucleotides employed had the following sequences and modifications:

**1<sub>15</sub>**, 5'-NH<sub>2</sub>-(T)<sub>20</sub>-CTG ATA AGT CGT CAA-3'

**1<sub>20</sub>**, 5'-NH<sub>2</sub>-(T)<sub>20</sub>-CTG ATA AGT CGT CAA CGT AT-3'

**1<sub>25</sub>**, 5'-NH<sub>2</sub>-(T)<sub>20</sub>-CTG ATA AGT CGT CAA CGT ATG CAA T-3'

**1<sub>30</sub>**, 5'-NH<sub>2</sub>-(T)<sub>20</sub>-CTG ATA AGT CGT CAA CGT ATG CAA TAT GCT-3'

**1<sub>35</sub>**, 5'-NH<sub>2</sub>-(T)<sub>20</sub>-CTG ATA AGT CGT CAA CGT ATG CAA TAT GCT CGC TT-3'

**1<sub>40</sub>**, 5'-NH<sub>2</sub>-(T)<sub>20</sub>-CTG ATA AGT CGT CAA CGT ATG CAA TAT GCT CGC TTA CTA A-3'

**1<sub>45</sub>**, 5'-NH<sub>2</sub>-(T)<sub>20</sub>-CTG ATA AGT CGT CAA CGT ATG CAA TAT GCT CGC TTA CTA ACT GGT-3'

**1<sub>50</sub>**, 5'-NH<sub>2</sub>-(T)<sub>20</sub>-CTG ATA AGT CGT CAA CGT ATG CAA TAT GCT CGC TTA CTA ACT GGT ATA GC-3'

**2<sub>P1</sub>**, 3'-GAC TAT TCA GCA GTT GCA TAC GTT ATA CGA GCG AAT GAT TGA CCA TAT CG-(T)<sub>6</sub>-5'-(Cy5)-5'-(T)<sub>6</sub>-AGA TAT GGT CAA TCA TTC GC-3'

**3<sub>P1</sub>**, 5'-biotin-(T)<sub>10</sub>-GCG AAT GAT TGA CCA TAT CT(Cy3)-3'

**2<sub>EcoRI</sub>**, 3'-GAC TAT TCA GCA GTT GCA TAC GTT ATA CGA GCG AAT GAT TGA CCA TAT CG-(T)<sub>6</sub>-5'-(Cy5)-5'-(T)<sub>6</sub>-AGA TAT GCG AAT TCA TTC GC-3'

**3<sub>EcoRI</sub>**, 5'-biotin-(T)<sub>10</sub>-GCG AAT GAA TTC GCA TAT CT(Cy3)-3'

**2<sub>p53DBD</sub>**, 3'-GAC TAT TCA GCA GTT GCA TAC GTT ATA CGA GCG AAT GAT TGA CCA TAT CG-(T)<sub>6</sub>-5'-(Cy5)-5'-(T)<sub>6</sub>-GAA CAT GTC CCA ACA TGT TG-3'

**3<sub>p53DBD</sub>**, 5'-biotin-(T)<sub>10</sub>-CAA CAT GTT GGG ACA TGT TCT(Cy3)-3'

#### 4. Analytical model of the BiFo-Chip measurements

In the following section we present the deduction of an analytical model for the BiFo-Chip. The central aspect of this model is based on the Bell-Evans model. The Bell-Evans model<sup>[4, 5]</sup> has been proven to accurately describe experimental results in the field of single molecule force spectroscopy in many different cases, such as the rupture of the biotin-streptavidin interaction.<sup>[6]</sup> Even though the Bell-Evans model is a two-state model, it has been shown that it describes to a first approximation very well more complex interaction patterns such as the unbinding of a hybridized dsDNA into two single DNA strands in a shear-geometry, a result which has been demonstrated experimentally multiple times.<sup>[7-9]</sup> Typically, the Bell-Evans model is used to analyze experimental data and extract the natural dissociation rate  $k_{off}$  and the potential width  $\Delta x$  for a certain molecular interaction.

Here, we approach the Bell-Evans model by inserting experimentally determined parameters  $\Delta x$  and  $k_{off}$  for the force-based dissociation of hybridized dsDNA oligomers in order to obtain the bond rupture probability density function  $p(f, \dot{f})$  for a given loading rate ( $\dot{f}$ ):

$$p(f, \dot{f}) = \frac{k_{off}}{\dot{f}} \cdot \exp\left(\frac{f \cdot \Delta x}{k_B T}\right) \cdot \exp\left(-\frac{k_{off}}{\dot{f}} \cdot \int_0^f du \cdot \exp\left(\frac{u \cdot \Delta x}{k_B T}\right)\right)$$

where  $k_B$  is the Boltzmann constant,  $T$  is the temperature and  $\dot{f} = df/dt$  is the loading rate.

In order to calculate  $p(f, \dot{f})$  for different long dsDNA oligomers, the corresponding  $\Delta x$  and  $k_{off}$  values must be known. In a previous study the correlation of  $\Delta x$  and  $k_{off}$  with the length of the dsDNA ( $n$  = number of base pairs) was experimentally characterized.<sup>[9]</sup> Thereby, they found the following relation for  $\Delta x$  and  $k_{off}$ :

$$k_{off}(n) = 10^{\alpha - \beta n} \cdot s^{-1} \quad \text{and} \quad \Delta x(n) = (t + n \cdot m) \cdot \text{\AA}$$

with  $\alpha = (3 \pm 1)$ ,  $\beta = (0.5 \pm 0.1)$ ,  $t = (7 \pm 3)$  and  $m = (0.7 \pm 0.3)$ .

Based on the Bell-Evans model and the relation between  $\Delta x$  and  $k_{off}$  with the number of base pairs, an analytical relation for NF can be deduced as follows. The molecular force probe consists of two dsDNA duplexes that are coupled in series. The probability with which one of the duplexes ruptures is measured by NF, and can be calculated from the overlap of the bond rupture probability density functions of the two DNA duplexes using the Bell-Evans model. Hereby, the NF is defined as the ratio of broken target bonds to the total amount of probed MFPs.

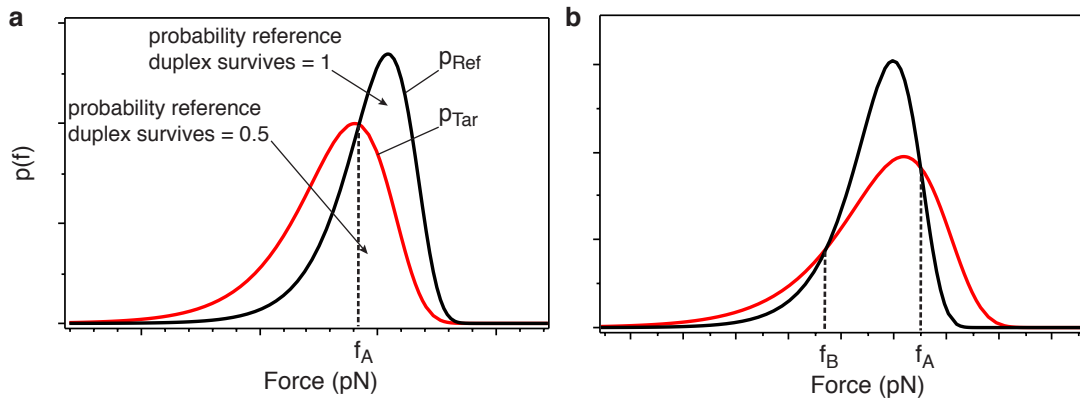


**Figure S1.** Calculated probability density functions. (a) Overlapping probability density functions with one intersection. (b) Arbitrary case with two intersections.

Figure S1 (a) shows an example for two overlapping probability density functions (e.g., 20 bp and 30 bp DNA duplexes). When the two probability density functions overlap, three areas can be distinguished (Figure S1 (a)); one area represents the probability that the reference duplex survives. In the overlap area, the probability that the reference duplex (respectively the target duplex) survives is 0.5. After some simplification steps, this can be expressed in the following mathematical equation:

$$NF(\dot{f}, n_R, n_T) = \frac{1}{2} \left[ 1 + \int_{f_A}^{\infty} df (p_{REF}(f, \dot{f}, n_R) - p_{TAR}(f, \dot{f}, n_T)) \right]$$

This equation describes the MFP without ligand (black dashed curve in Figure 2 and Figure 3), since in this case the two probability density functions have only one intersection ( $n_T(n_R) =$  number of base pairs of the target (reference) duplex). A generalization for arbitrary parameters  $\Delta x$  and  $k_{off}$ , which can result in probability density functions with two intersections (see Figure S1 (b)), is fulfilled by the following equation:

$$NF(\dot{f}, n_R, n_T) = \frac{1}{2} \left[ 1 + \int_{f_A}^{\infty} df (p_{REF}(f, \dot{f}, n_R) - p_{TAR}(f, \dot{f}, n_T)) + \int_{f_B}^{\infty} df (p_{REF}(f, \dot{f}, n_R) - p_{TAR}(f, \dot{f}, n_T)) \right]$$

In the case of only one intersection (i.e.  $f_B = 0$ ), this equation simplifies to the previous one. Finally, the applied loading rate must be determined before the NF can be calculated. This was already described in detail by Albrecht et al.<sup>[10]</sup> Briefly, since the PDMS-stamp is elastic,

the stamp deforms in the separation process, which results in a vertical separation velocity acting on the MFPs that is different from the applied one. In order to assess the applied loading rate, the stamp-chip separation process is recorded on the inverted microscope. Stamp-chip contact areas are separated at the edge of a propagating cleft at which the MFPs are loaded and ruptured. Interference patterns emerge after separation behind the moving cleft, which allow measurement of the angle of the propagating cleft between stamp and chip. This angle translates the measured lateral separation velocity into a vertical separation velocity, which acts directly on the MFPs. By knowing the separation velocity acting on the MFPs, and the length of the PEG- and poly-t-spacer that define the spring constant of the system, the most probable loading rate can be estimated as described earlier.<sup>[10]</sup> Here, we applied in all measurements a separation velocity of  $5 \mu\text{m s}^{-1}$  on the PDMS-stamp, which resulted on average in a most probable loading rate of  $1.43 \times 10^6 \text{ pN s}^{-1}$ .

We applied the NF-model to the measured BiFo-chip data. Fitting the values for  $\alpha$ ,  $\beta$ ,  $t$  and  $m$  resulted in the optimized curve progression shown in Figures 2 and 3 ( $\alpha = 2.8$ ,  $\beta = 0.48$ ,  $t = 6.4$  and  $m = 0.76$ ). The values  $\alpha$ ,  $\beta$ ,  $t$  and  $m$  are within the error bars of the values determined by Strunz et al.<sup>[9]</sup> The fitted values for  $\alpha$  and  $\beta$  are slightly lower than those obtained by Strunz et al., which reflects a lower dependence of  $k_{off}$  on the number of base pairs.  $\Delta x$  showed a slightly higher base pair-dependence. This may be due to the fact that the DNA duplexes used for BiFo-Chip have a GC-content of 40% to 42%, while the DNA oligomers used by Strunz et al. had a GC-content of around 60% to 65%. Furthermore, in the article by Strunz et al., only 3 different oligomers were investigated, while the BiFo-Chip uses 8 different long reference duplexes, which should allow a more precise measurement.

[1] P. M. D. Severin, D. Ho, H. E. Gaub, *Lab Chip* **2011**, *11*, 856-862.

[2] D. Ho, C. Dose, C. H. Albrecht, P. M. D. Severin, K. Falter, P. B. Dervan, H. E. Gaub, *Biophys. J.* **2009**, *96*, 4661-4671.

[3] C. H. Albrecht, H. Clausen-Schaumann, H. E. Gaub, *Journal of Physics: Condensed Matter* **2006**, *18*, 581-599.

[4] G. I. Bell, *Science* **1978**, *200*, 618-627.

[5] E. Evans, K. Ritchie, *Biophys. J.* **1999**, *76*, 2439-2447.

[6] R. Merkel, P. Nassoy, A. Leung, K. Ritchie, E. Evans, *Nature* **1999**, *397*, 50-53.

[7] J. Morfill, F. Kuehner, K. Blank, R. A. Lugmaier, J. Sedlmair, H. E. Gaub, *Biophys. J.* **2007**, *93*, 2400-2409.

- [8] P. M. D. Severin, X. Zou, H. E. Gaub, K. Schulten, *Nucleic Acids Research* **2011**, *39*, 8740-8751.
- [9] T. Strunz, K. Oroszlan, R. Schäfer, H. J. Güntherodt, *Proc. Natl. Acad. Sci. USA* **1999**, *96*, 11277-11282.
- [10] C. H. Albrecht, G. Neuert, R. A. Lugmaier, H. E. Gaub, *Biophys. J.* **2008**, *94*, 4766-4774.